Effect of Polydispersity on Viscoelasticity and Shear Thickening in Aqueous Solutions of Hydrocarbon End-Capped Poly(ethylene oxide)

Sharon X. Ma[†] and Stuart L. Cooper*[,‡]

Department of Chemical Engineering, University of Delaware, Newark, Delaware 19716

Received March 5, 2001; Revised Manuscript Received December 26, 2001

ABSTRACT: The linear viscoelastic and shear thickening behavior in aqueous solutions of model hydrophobically end-capped poly(ethylene oxide) were examined. Comparisons are made between monodisperse samples, unimodal polydisperse samples, and bimodal polydisperse samples. While the linear viscoelastic behavior is qualitatively similar for both polydisperse and monodisperse systems, the steady shear response displayed a marked dependence on the type of polydispersity, especially in the shear thickening behavior. No significant shear thickening was observed in unimodal polydisperse samples, and one possible explanation for this lack of significant shear thickening could be due to a lack of cooperative non-Gaussian chain stretching.[1] Samples with bimodal molecular weight distribution exhibit similar shear thickening behavior as monodisperse samples. Furthermore, the characteristics of shear thickening of the bimodal system were found to be the same as in the monodisperse polymer with the lower molecular weight (10K), instead of that of the monodisperse polymer with the same average molecular weight (20K). The mechanism of shear thickening is due to the non-Gaussian chain stretching of the shorter polymer chain.

Introduction

Hydrophobically end-capped poly(ethylene oxide) (PEO) belongs to a wider class of polymeric materials—associating polymers. Associating polymers are polymers that contain small amounts of functional groups that are capable of forming multiplets in a selective solvent. These materials are industrially important since they can be tailored to exhibit specific rheological properties and have found wide applications in coatings, paper manufacture, oil production and transportation, water treatments, and thickeners for food and health care products. Hydrophobically end-capped PEO is an ideal system for fundamental studies of associating polymers due to the simplicity of its structure and known position of associating groups (i.e., at both ends of the polymer chain). The presence of the hydrophobic end groups gives rise to unusual rheological behavior such as enhanced zero-shear viscosity and more elastic behavior. Numerous studies have established that the unusual rheological behavior of associating polymers originates from the formation of a physically cross-linked network.[2−12] Shear-thickening behavior has also been reported in associating polymer solutions, including ionomers in nonpolar solvents[13−20] and hydrophobically end-capped PEO in aqueous solutions and similar systems.[2,21−28]

In a separate study, we have reported on a systematic study of shear thickening behavior of hydrocarbon end-capped PEO in aqueous solutions.[29] The effects of polymer concentration, temperature, association strength, and polymer chain length on shear thickening were investigated. It was found that aqueous solutions of hydrophobically end-capped PEO with higher molecular weight (35 000) show only shear thinning behavior whereas solutions of PEO with lower molecular weights (10 000 and 20 000) show mild shear thickening over a range of concentrations. The magnitude of shear thickening was found to increase with association strength and to decrease with temperature. The critical shear rate (shear rate at which shear thickening occurs) shifted to lower shear rate as the association strength or concentration increased or as temperature decreased. The scaling factors of the magnitude of shear thickening and the critical shear rate and the shear stress have been interpreted in terms of the free path model proposed by Marrucci et al.,[1] which suggests that shear thickening is due to non-Gaussian chain stretching and fast recapture of dissociated end groups. In this paper, we continue our study by examining the effect of polydispersity on the rheological properties of associating polymer solutions, especially shear thickening behavior.

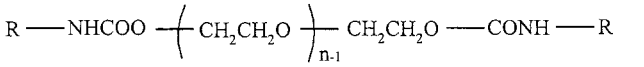

Figure 1. Chemical structure of model systems (hydrocarbon end-capped PEO).

Experimental Section

Materials. The detailed description of synthesis of the model systems is reported elsewhere.[29] The structure of materials is shown in Figure 1. The materials used in this study are summarized in Table 1.

Sample Preparation. Solutions at different concentration levels were prepared by directly dissolving a known amount of polymer into deionized distilled H_2O (Nanopure, resistance above 17 Ω·cm). Each solution was gently stirred until the solution was homogeneous. When the viscosity of solution was too high to be efficiently stirred, it was gently rotated for 2 or 3 days, depending on the viscosity.

Rheological Measurement. The rheological properties of the polymer solutions were measured using a Bohlin VOR strain-controlled rheometer with a Couette geometry (C14, 14

[†] Present address: Department of Chemistry, University of California—Irvine, Irvine, CA 92697.

[‡] Present address: North Carolina State University, Campus Box 7101/109 Holladay Hall, Raleigh, NC 27695-7101.

10.1021/ma010390p CCC: $22.00
Published on Web 02/16/2002

Table 1. Molecular Weight and Polydispersity of Polymers Used in This Study

designation	M_n	polydispersity	hydrophobe per chain
PEO(35K,m)-C18	35 000	1.15	2
PEO(20K,m)-C18	20 000	1.03	2
PEO(10K,m)-C18	10 000	1.02	2
PEO(20K,p)-C18	20 000[a]	1.50	2
PEO(20K,b)-C18	20 000[b]	1.38	2
PEO(14K,b)-C18	14 000[c]	1.43	2

[a] The molecular weight distribution is a typical Gaussian distribution. [b] The polymer was made from 40% (mole fraction) of PEO(35K,m)-C18 and 60% (mole fraction) of PEO(10K,m)-C18. The number- and weight-average molecular weight are then calculated by $\overline{M_n} = \sum x_i M_i$ and $\overline{M_w} = \sum w_i M_i = \sum(x_i M_i/\sum x_i M_i)M_i$. [c] The polymer was made from 16% (mole fraction) of PEO(35K,m)-C18 and 84% (mole fraction) of PEO(10K,m)-C18. The weight-average molecular weight is 20 000.

mm o.d. with a gap of 1 mm) or cone and plate (CP5/30, 3 cm, 5° cone) at temperatures ranging from 5 to 40 °C. Both steady-shear and oscillatory tests were conducted on each sample at each temperature. A standard procedure was used for all rheological measurements. After loading, the sample was sheared for 2 min at 1 s^{-1}, followed by 15 min of rest. This ensures that all samples are in equilibrium structure if there is any nonequilibrium structure introduced by sample loading. A strain sweep experiment was performed prior to each oscillatory experiment to determine the linear viscoelasticity regime. For the steady shear experiment, an equilibration time of 90 s was given at each shear rate to allow the system to reach steady state.

Results and Discussion

Broad Molecular Weight Distribution. *Linear Viscoelastic Behavior.* The dynamic experiments probe the equilibrium structure and relaxation spectrum of the material. It has been observed that despite the complexity of shear behavior, the viscoelastic behavior of telechelic associating polymers is quite simple, even for polymers with broad molecular weight distribution.[2,21] The Maxwell model with a single relaxation time usually is sufficient to describe the viscoelastic data.

$$G'(\omega) = G_\infty\left(\frac{\omega^2\tau^2}{1+\omega^2\tau^2}\right) \quad (1)$$

$$G''(\omega) = G_\infty\left(\frac{\omega\tau}{1+\omega^2\tau^2}\right) \quad (2)$$

where ω is the angular frequency, G_∞ is the plateau modulus, and τ is the relaxation time.

Figure 2 shows the storage modulus G' and loss modulus G'' of octadecyl end-capped PEO (average molecular weight of 20 000) with a unimodal polydispersity of 1.03 and 1.5. Two systems show qualitatively similar behavior: slopes of approximately 2 and 1 were observed for the storage (G') and loss modulus (G'') at low frequencies, respectively; G' and G'' cross over at higher frequency, indicating the formation of a transient network. The Maxwell model with a single relaxation time is sufficient to describe the experimental data from both samples (shown as solid lines). The simple Maxwellian fluid behavior suggests that in telechelic associating polymer solutions the stress relaxation mechanism is the detachment of an end group from the hydrophobic junction. Plazek and Frund[30] observed a long-time terminal dispersion at lower frequencies (log

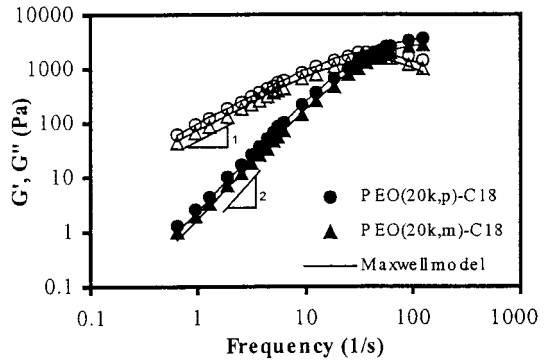

Figure 2. Dynamic modulus of hydrophobically end-capped PEO(20 000) with polydispersity of 1.03 and 1.5.

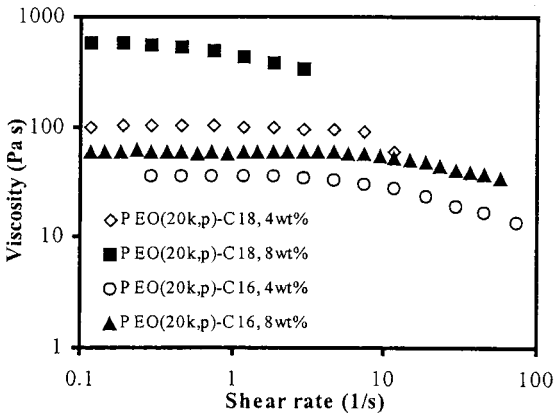

Figure 3. Typical steady shear viscosity profile of hydrophobically end-capped PEO with polydispersity of 1.5.

$\omega \leq 0.5$) in a similar system. However, the frequency studied here is not low enough to observe the long-time process.

Shear Thickening Behavior. An interesting rheological behavior exhibited by hydrophobically end-capped PEO solutions is the so-called shear thickening phenomenon (i.e., viscosity increases with shear rates). Several mechanisms have been proposed to explain shear thickening behavior observed in associating polymer solutions. These includes shear-induced "cross-linking" and shear-induced non-Gaussian chain stretching.

Figure 3 shows steady shear viscosity profiles of aqueous solution of hydrophobically end-capped PEO-(20K) with a unimodal polydispersity of 1.5. Unlike solutions of monodisperse PEO chains, no significant shear thickening is observed in the polydisperse samples. Jenkins[24] and Annable et al.[2] reported shear thickening in similar systems at lower concentrations. The different observation might be due to the differences in the polymer structure. As reported previously,[29] shear thickening is a result of the cooperative effect of non-Gaussian chain stretching. In a unimodal polydisperse sample, the bridges are composed of polymer chains with different molecular weight. At any particular deformation (or shear rate), some bridges (low molecular weight) are highly stretched, while some are still well inside Gaussian region. As shear rate increases, when the chains with high molecular weight are finally stretched into the non-Gaussian region, the chains with low molecular weight have most likely broken free from the junctions. There is no unique shear rate where most of bridges are stretched into the non-Gaussian region to give rise to the shear thickening effect. In the case of a monodisperse sample most of the bridges are stretched

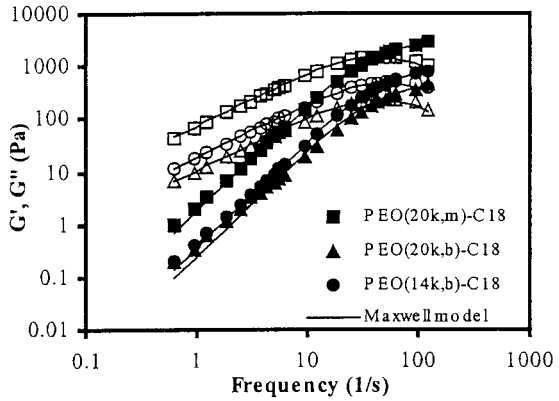

Figure 4. Dynamic modulus of 4 wt % of octadecyl end-capped PEOs with monodisperse and bimodal molecular weight distribution at 20 °C. The solid symbols are G', and open symbols are G''.

to a similar extent. When the association strength is high enough to allow non-Gaussian chain stretching, shear thickening occurs.

In summary, hydrophobically end-capped PEO with a broad unimodal molecular weight distribution shows qualitatively similar viscoelastic behavior as monodisperse samples. The Maxwell model with a single relaxation time is sufficient to describe the viscoelastic response. This suggests that a similar network structure was formed in both polydisperse and monodisperse samples. However, the steady shear response of the two systems is quite different. Unlike the monodisperse samples, the polydisperse samples in general show Newtonian behavior at low shear rates and shear thinning behavior at high shear rates. The lack of shear thickening in the unimodal polydisperse samples can be explained by a lack of cooperative non-Gaussian chain stretching. To gain more insight into the mechanism of shear thickening in associating polymer solutions, a study on system with bimodal molecular weight distribution is presented below.

Bimodal Molecular Weight Distribution. As shown above, polydispersity has a significant effect of the rheological properties of associating polymer solutions, especially on shear thickening behavior. To further reveal on the mechanism of shear thickening in aqueous solutions of associating polymers, a system with bimodal molecular weight distribution was studied. The system consists of a mixture of octadecyl end-capped monodisperse PEOs with molecular weight of 10 000 and 35 000. Two samples were made: one with a number-average molecular weight of 20 000 and the other one with a weight-average molecular weight of 20 000. The composition and designation of the two samples are listed in Table 1. The rheological experiments were carried out the same way as on the monodisperse samples.

Linear Viscoelastic Behavior. Figure 4 shows dynamic modulus of 4 wt % of octadecyl end-capped PEOs with monodisperse and bimodal molecular weight distribution at 20 °C. The bimodal MW distribution samples show qualitatively similar behavior as monodisperse samples. Namely, at low frequencies, G' and G'' exhibit terminal behavior, and at high frequencies, G' crosses over G'' and approaches a plateau value. Unlike the solutions of mixed polymers with different end groups in Annable et al.'s study,[21] a single-mode Maxwell model (shown in the solid lines) adequately describes the experimental data at all concentrations studied. This

Table 2. G_∞ and τ Determined by the Maxwell Model

concn (wt %)	materials	G_∞ (Pa)	τ (s)
8	PEO(20K,m)-C18	7.98E+03[a]	0.090
	PEO(20K,b)-C18	1.49E+03	0.035
	PEO(14K,b)-C18	4.33E+03	0.028
6	PEO(20K,m)-C18		
	PEO(20K,b)-C18	9.72E+02	0.029
	PEO(14K,b)-C18	2.61E+03	0.024
4	PEO(20K,m)-C18	2.97E+03	0.024
	PEO(20K,b)-C18	4.24E+02	0.027
	PEO(14K,b)-C18	9.53E+02	0.020
3	PEO(20K,m)-C18	1.14E+03	0.020
	PEO(0K,b)-C18	2.33E+02	0.018
	PEO(14K,b)-C18	2.28E+02	0.017

[a] Read as 7.98×10^3.

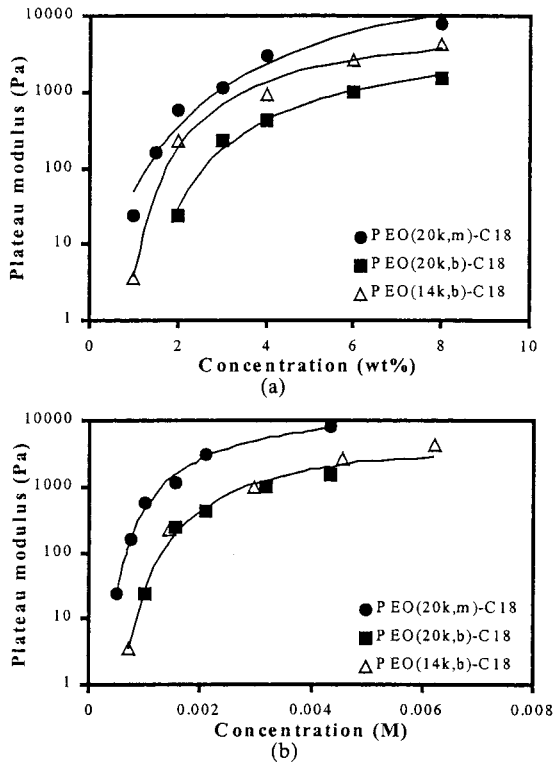

Figure 5. Effect of concentration on plateau modulus of octadecyl end-capped PEO with bimodal molecular weight distribution: (a) concentration by weight; (b) concentration molar units.

implies that the linear viscoelastic response of these polymer solutions is governed by the dissociation of the end groups from the network junctions. The single polymer chain relaxation is negligible in these systems. Relaxation time (τ) and plateau modulus (G_∞) data are summarized in Table 2.

As concentration increases, both G' and G'' increase, and the crossover shifts to lower frequencies as observed in monodisperse and polydisperse samples. The plateau modulus increases with concentration as well (Table 2). More data at higher frequencies are needed to draw any conclusion on the effect of concentration on the length of the plateau region.

The concentration dependence of the plateau modulus is shown in Figure 5. The plateau modulus increases rapidly with concentration in the low concentration regime and tends to level off at higher concentrations, similar to that of monodisperse samples. G_∞ of the two samples with bimodal molecular weight distribution are lower than that of the monodisperse sample at the same

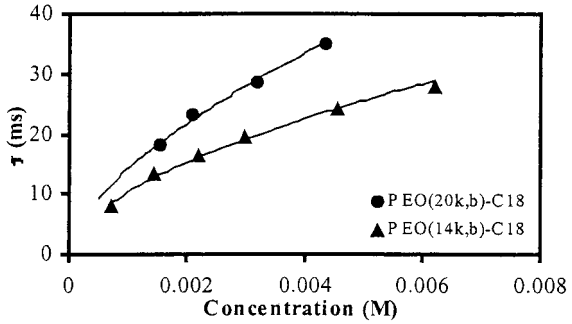

Figure 6. Effect of concentration on relaxation time of octadecyl end-capped PEO with bimodal molecular weight distribution (concentration by mole).

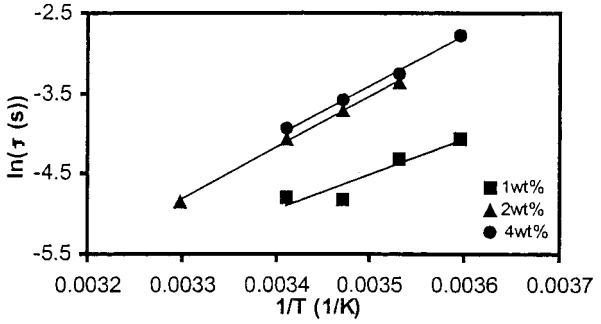

Figure 7. Effect of temperature on relaxation time of octadecyl end-capped PEO with bimodal molecular weight distribution (average molecular weight of 20K).

concentration, and the plateau modulus of PEO(14K,b)-C18 is slightly higher than that of PEO(20K,b)-C18 at the same concentration by weight (Figure 5a). However, it should be noted that at the same weight concentration the molar concentration of PEO(14K,b)-C18 is actually higher than that of PEO(20K,b)-C18 due to the difference in molecular weight. When plotted against molar concentration, G_∞ of the two samples falls onto single curve, indicating that similar structures formed in two samples (Figure 5b).

The concentration dependence of the relaxation time is shown in Figure 6. It can be seen that the relaxation time increases with concentration, similar to that of monodisperse samples. The relaxation time of samples with a bimodal MW distribution is smaller than that of monodisperse samples with the same number-average molecular weight (Table 2). Figure 7 shows an Arrhenius type of temperature dependence of relaxation time. This again provides clear evidence that a single process underlies the relaxation kinetics in solutions of associating polymers, as found in monodisperse samples and other studies. The apparent activation energy estimated from the relaxation time is 37, 52, and 53 kJ/mol for 1, 2, and 4 wt % concentrations, respectively. Above 2 wt %, the apparent activation energy remains nearly constant, indicating that the transient network structure has fully developed. The linear viscoelastic data are consistent with the steady shear in that the zero-shear viscosity $\eta_0 = G_\infty\tau$ within 10%.

Shear Thickening Behavior. The steady shear response of the octadecyl end-capped PEOs with bimodal MW distribution is qualitatively similar to that of monodisperse samples of the molecular weight of 20 000. The viscosity profile is characterized by an extended Newtonian plateau at low shear rates, followed by shear thickening at moderate shear rates and shear thinning at high shear rates. Even though shear thickening is

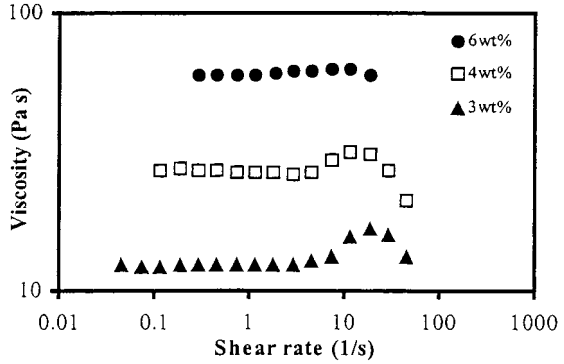

Figure 8. Effect of concentration on shear thickening in octadecyl end-capped PEO (20K) with bimodal molecular weight distribution.

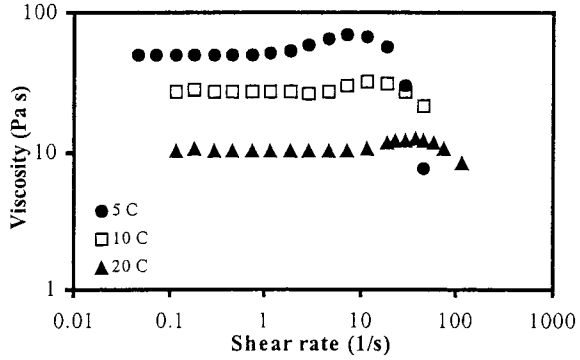

Figure 9. Effect of temperature on shear thickening in octadecyl end-capped PEO (20K) with bimodal molecular weight distribution.

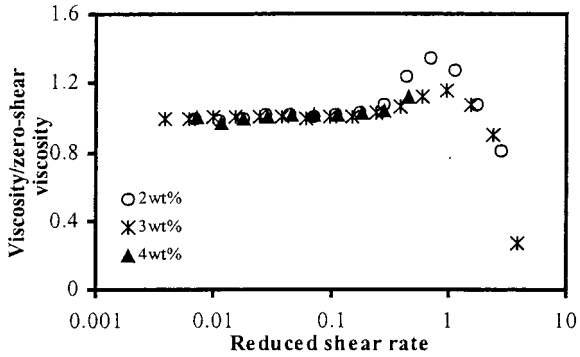

Figure 10. Steady shear viscosity (normalized by zero-shear viscosity) of PEO(14 k,b)-C18 as a function of reduced shear rate at 2, 3, and 4 wt %.

absent in the unimodal polydisperse sample, samples with the same average molecular weight (either number or weight average) but with a bimodal distribution clearly exhibit shear thickening. Figures 8 and 9 show the effect of concentration and temperature on shear thickening, respectively. The onset of shear thickening and shear thinning shifts to lower shear rates as concentration increases or temperature decreases, similar to that observed in monodisperse samples.

Figure 10 plots the viscosity of PEO(14K,b)-C18 as a function of reduced shear rate (shear rate times the relaxation time). As observed in monodisperse samples, the critical reduced shear rate in samples with bimodal molecular weight distribution is independent of concentration. (The critical reduced shear rates are around 0.2 for all samples plotted.) This is consistent with the prediction of the free path model where, for systems with the same molecular weight, the critical reduced

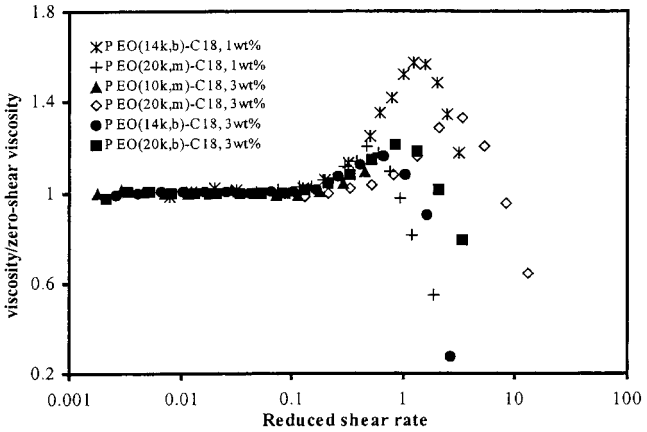

Figure 11. Steady shear viscosity (normalized by zero-shear viscosity) of 3 wt % of PEO(20K,m)-C18, PEO(20K,b)-C18, and PEO(14K,b)-C18 as a function of reduced shear rate.

shear rate should be roughly the same regardless of concentration.[29]

Figure 11 plots the steady shear viscosity (normalized by zero-shear viscosity) as a function of reduced shear rate ($\dot{\gamma}\tau$). There are two concentration regimes where the shear thickening displays a different signature. Below the overlap concentration (about 2 wt %) the onset of shear thickening occurs at almost the same shear rate for both PEO(14K,b)-C18 and PEO(20K,m)-C18 (cross symbols in Figure 11), while above the overlap concentration, the onset of shear thickening of both PEO(20K,b)-C18 and PEO(14K,b)-C18 occurs at lower shear rates than those of PEO(20K,m)-C18.

Several groups have proposed that shear thickening is due to the shear-induced interchain association at the expense of intrachain association. If shear thickening is a result of such a shear-induced transition, one would expect two samples of the same molecular weight but with different polydispersities to exhibit qualitatively similar shear thickening behavior. The effect of polydispersity would only manifest itself through a broadening effect (i.e., the onset of shear thickening occurs over a wider range of shear rates). This mechanism seems to agree with our experimental results at concentrations below the overlap concentration. The zero-shear viscosity of the PEOs below the overlap concentration is much smaller. The fraction of elastically active chains (ν/n) is extremely small, less than 10%. This implies that below the overlap concentration intramolecular association dominates, and the network has not yet fully developed. In this case, the shear thickening observed may be due to the shear-induced transition from intra- to intermolecular association. However, above the overlap concentration where the network is fully developed, this mechanism can no longer rationalize the shear thickening behavior observed.

The experimental observation at higher concentrations (≥2 wt %), however, is consistent with the non-Gaussian chain stretching mechanism. The free path model predicts that the critical shear rate (the shear rate at onset of shear thickening) is proportional to $N^{1/2}$ (N is the molecular weight of the polymer).[1] It can be readily seen in Figure 11 that the critical reduced shear rate of PEO(20K,b)-C18 is smaller than that of PEO-(20K,m)-C18 but similar to that of PEO(10K,m)-C18. We reported previously that PEO(35K,m)-C18 does not show shear thickening due to the unobtainable large deformation required to stretch the "bridges" into the non-Gaussian regime to give rise to shear thickening. Therefore, in the PEO(20K,b)-C18 sample, the "bridges" with smaller molecular weight (10K) are stretched when subjected to shear flow. When these "bridges" are stretched into non-Gaussian regime, shear thickening occurs. The deformation required to do so is expected to be similar to that for PEO(10K,m)-C18. Thus, the critical reduced shear rate is similar for the PEO(20K,b)-C18 and PEO(10K,m) samples. Furthermore, the two bimodal molecular weight samples have similar critical reduced shear rate regardless of the difference in average molecular weight. If the shear thickening in samples with bimodal molecular weight distribution results from the non-Gaussian stretching of the shorter polymer chains (molecular weight of 10 000), then the two samples will exhibit similar characteristics of shear thickening despite the macroscopic difference in the average molecular weight.

Conclusions

The effect of polydispersity on viscoelasticity and shear thickening of hydrophobically end-capped PEO has been studied. Aqueous solutions of hydrophobically end-capped PEO with broad or bimodal molecular weight distribution show qualitatively similar viscoelastic behavior as monodisperse samples. The Maxwell model with a single relaxation time is sufficient to describe the viscoelastic response. This suggests that similar network structures are formed in both polydisperse and monodisperse samples. However, the steady shear response displayed a marked dependence on polydispersity, especially in the shear thickening behavior. Unlike the monodisperse samples, the unimodal polydisperse samples in general show Newtonian behavior at low shear rates and shearing thinning behavior at high shear rates (no shear thickening was observed). The lack of shear thickening in unimodal polydisperse samples can be explained by a lack of cooperative non-Gaussian chain stretching. Samples with bimodal molecular weight distribution, consisting of two monodisperse polymers (10K and 35K), exhibit similar shear thickening behavior as monodisperse samples of the same average molecular weight. Furthermore, the characteristics of shear thickening of the bimodal systems were found to be the same as in the monodisperse polymer with the lower molecular weight (the 10K component of the bimodal polymer mixture), instead of that of the monodisperse polymer with the same average molecular weight (20K). The mechanism of shear thickening is due to the non-Gaussian chain stretching of the shorter polymer chain.

Acknowledgment. This work has been supported by the National Science Foundation under Grant DMR-9815942.

References and Notes

(1) Marrucci, G.; Bhargava, S.; Cooper, S. L. *Macromolecules* **1993**, *26*, 6483−6488.
(2) Annable, T.; Buscall, R.; Ettelaie, R.; Whittlestone, D. *J. Rheol.* **1993**, *37*, 695−726.
(3) Ng, W. K.; Tam, K. C.; Jenkins, R. D. *J. Rheol.* **2000**, *44*, 137−147.
(4) Winnik, M. A.; Yekta, A. *Curr. Opin. Colloid Interface Sci.* **1997**, *2*, 424−436.
(5) Alami, E.; Almgren, M.; Brown, W.; Francois, J. *Macromolecules* **1996**, *29*, 2229−2243.
(6) Chassenieux, C.; Nicolai, T.; Durand, D. *Macromolecules* **1997**, *30*, 4952−4958.

(7) Chassenieux, C.; Nicolai, T.; Durand, D.; Francois, J. *Macromolecules* **1998**, *31*, 4035−4037.
(8) Francois, J.; Maitre, S.; Rawiso, M.; Sarazin, D.; Beinert, G.; Isel, F. *Colloids Surf. A: Physicochem. Eng. Aspects* **1996**, *112*, 251−265.
(9) Tanaka, F.; Edwards, S. F. *J. Non-Newtonian Fluid Mech.* **1992**, *43*, 247.
(10) Rubinstein, M.; Dobrynin, A. V. *TRIP* **1997**, *5*, 181−186.
(11) Pham, Q. T.; Russel, W. B.; Thibeault, J. C.; Lau, W. *Macromolecules* **1999**, *32*, 2996−3005.
(12) Pham, Q. T.; Russel, W. B.; Thibeault, J. C.; Lau, W. *Macromolecules* **1999**, *32*, 5139−5146.
(13) Bhagarva, S.; Cooper, S. L. *Macromolecules* **1998**, *31*, 508−514.
(14) Bhargava, S. Ph.D. Thesis In *Chemical Engineering*; University of Delaware: Newark, DE, 1997.
(15) Broze, G.; Jerome, R.; Teyssie, P.; Marco, C. *Macromolecules* **1983**, *16*, 996−1000.
(16) Chassenieus, C.; Tassin, J.-F.; Gohy, J.-F.; Jerome, R. *Macromolecules* **2000**, *33*, 1796−1800.
(17) Lundberg, R. D.; Duvdevani, I. *Polym. Mater. Sci. Eng.* **1989**, *61*, 259.
(18) Lundberg, R. D.; Duvdevani, I. In *Polymers as Rheology Modifiers*; Schulz, D. N., Glass, J. E., Eds.; ACS Symposium Series 462; American Chemical Society: Washington, DC, 1991; pp 155−175.
(19) Maus, C.; Fayt, R.; Jerome, R.; Teyssie, P. *Polymer* **1995**, *36*, 2083−2088.
(20) Peiffer, D. G.; Kaladas, J.; Duvdevani, I.; Higgins, J. S. *Macromolecules* **1987**, *20*, 1397.
(21) Annable, T.; Buscall, R.; Ettelaie, R. *Colloids Surf. A: Physicochem. Eng. Aspects* **1996**, *112*, 97−116.
(22) Evans, G. T. *J. Chem. Phys.* **1998**, *108*, 1570−1577.
(23) Hu, Y.; Wang, S. Q.; Jamieson, A. M. *J. Rheol.* **1993**, *37*, 531−545.
(24) Jenkins, R. D. In *Chemical Engineering*; Lehigh University: Bethlehem, 1990.
(25) Kaczmarski, J. P.; Glass, J. E. *Macromolecules* **1993**, *26*, 5149−5156.
(26) Kaczmarski, J. P.; Glass, J. E. *Langmuir* **1994**, *10*, 3035−3042.
(27) English, R. J.; Gulati, H. S.; Jenkins, R. D.; Khan, S. A. *J. Rheol.* **1997**, *41*, 427−444.
(28) Lundberg, D. J.; Glass, J. E.; Eley, R. R. *J. Rheol.* **1991**, *35*, 1255−1274.
(29) Ma, S. X.; Cooper, S. L. *Macromolecules* **2001**, *34*, 3294−3301.
(30) Plazek, D.; Frund, Z. *J. Rheol.* **2000**, *44*, 929−948.

MA010390P